Journal of Organometallic Chemistry, 371 (1989) 233–246
Elsevier Sequoia S.A., Lausanne – Printed in The Netherlands
JOM 09903

The synthesis from related methylgermyliron carbonyl precursors, of two doubly-bridged metal–metal bonded compounds, $[\mu\text{-Ge}\{Co(CO)_4\}Me]_2Co_2(CO)_6$ and $[\mu\text{-Ge}\{Co(CO)_4\}Me]_2Fe_2(CO)_7$, and their crystal structures

Skelte G. Anema, Kenneth M. Mackay * and Brian K. Nicholson *

School of Science, University of Waikato, Private Bag, Hamilton (New Zealand)

(Received February 10th, 1989)

Abstract

$Co_2(CO)_8$ reacts with $[Fe(CO)_4(GeMeH_2)_2]$ to form $[\mu\text{-Ge}\{Co(CO)_4\}Me]_2Co_2(CO)_6$ (**5**) as the major identified product, and with $[\{Fe(CO)_4(GeMeH)\}_2]$ to give $[\mu\text{-Ge}\{Co(CO)_4\}Me]_2Fe_2(CO)_7$ (**6**) in high yield. X-ray diffraction studies show a close relationship between **5** and **6**, each having two Ge[Co(CO)$_4$]Me groups replacing two bridging CO ligands in the parent dimetal carbonyls, respectively $Co_2(CO)_8$ and $Fe_2(CO)_9$. In the GeM_2 triangles, while Ge–Co, at 2.397 Å, and, Ge–Fe at 2.451 Å, are little changed from those for related species, the metal–metal bonds are lengthened by more than 0.2 Å, compared with those in the parent carbonyls, to 2.733 Å for Co–Co and 2.693 Å for Fe–Fe.

Introduction

The reaction with $Co_2(CO)_8$ of H–Ge–metal species often forms interesting clusters which retain the Ge–metal bond, as in the reactions shown in equations 1 [1] and 2 [2,3].

$$[(CO)_5MnGeH_3] + Co_2(CO)_8 \rightarrow [\{(CO)_5Mn\}GeCo_3(CO)_9] \quad (1)$$

$$[Fe(CO)_4GeH_2] + Co_2(CO)_8 \rightarrow [\{(CO)_7Co_2\}Ge]_2Fe_2(CO)_7 \quad (2)$$

Bis(methylgermyl)tetracarbonyliron (**1**) is readily formed by a coupling reaction, and slowly condenses [4] to the four-membered ring species **2** (eq. 3).

$$2\,[Fe(CO)_4(GeMeH_2)_2] \rightarrow [\{Fe(CO)_4(GeMeH)\}_2] + 2\,GeMeH_3 \quad (3)$$
(**1**) (**2**)

In this study, the contrasting reactions with $Co_2(CO)_8$ of these two related methylgermyliron compounds, **1** and **2**, are reported. In the main isolated product from the reaction of **1** the Fe–Ge bonds have been cleaved, whereas they are retained in the sole product from **2**.

0022-328X/89/$03.50

Results

$[Fe(CO)_4(GeMeH_2)_2]$ (1) plus $Co_2(CO)_8$. The reactions carried out at low temperature gave ^1H NMR signals from a number of products but indicated the formation of $HCo(CO)_4$ in substantial ratio. The mass spectra of the product mixtures demonstrated the presence of at least three major components. At the lowest inlet temperature, only ions assignable to a compound of formula $Me_2Ge_2FeCo_2(CO)_8$ (**3**) were present. At higher inlet temperatures, and in the less soluble fractions, there were also present the known [5,6] compound $[\mu\text{-}Ge\{Co(CO)_4\}Me]Co_2(CO)_7$ (**4**) and the compound characterised below as $[\mu\text{-}Ge\{Co(CO)_4\}Me]_2Co_2(CO)_6$ (**5**). Other species found in the mass spectra were unidentified, or were decarbonylation products of **4** or **5**. The detection of **3** depended on fractional sublimation in the mass spectrometer, and efforts to obtain a bulk sample have so far been unsuccessful. It is transformed in part into **4** or **5**.

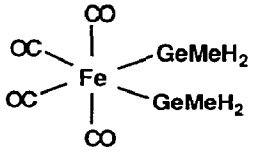

1

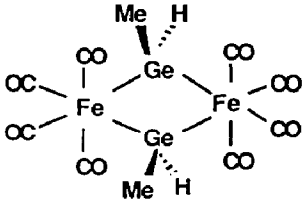

2

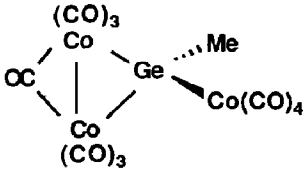

4

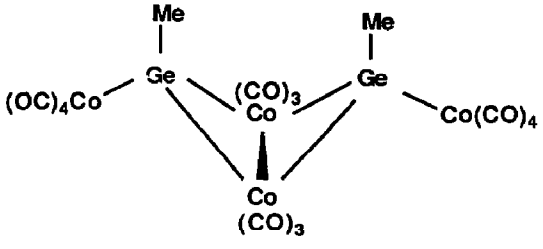

5

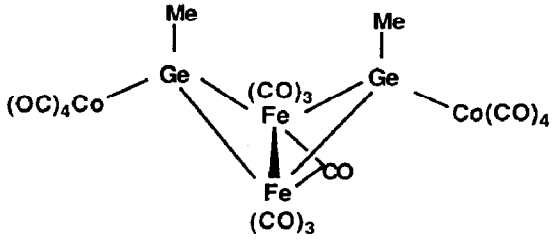

6

In the reaction in solution at room temperature, **3** was not observed, and **5** was the main component in the product mixture. On the scale used the cleanest work-up came after a reaction time of about 2 h, when the total gas evolution was > 80% and gave some 50% of **5**. The main effect of longer reaction times was the formation of a higher proportion of $Co_4(CO)_{12}$ (probably from $HCo(CO)_4$) which led to difficulties in separation and a lower recovery of all the products. The overall reactions are indicated by equations 4 and 5:

$$\underset{(1)}{[Fe(CO)_4(GeMeH_2)_2]} + 2Co_2(CO)_8 \rightarrow \underset{(5)}{[\mu\text{-}Ge\{Co(CO)_4\}Me]_2Co_2(CO)_6} + \text{"}Fe(CO)_4\text{"} + 2H_2 + 2CO \quad (4)$$

$$\underset{(1)}{[Fe(CO)_4(GeMeH_2)_2]} + 3Co_2(CO)_8 \rightarrow 2\underset{(4)}{[\mu\text{-}Ge\{Co(CO)_4\}Me]Co_2(CO)_7} + \text{"}Fe(CO)_4\text{"} + 2H_2 + 2\,CO \quad (5)$$

The fate of the "$Fe(CO)_4$" was not established in the room temperature solution reactions: a proportion appeared as $Fe(CO)_5$. The lower temperature reactions suggested that **3** is the major Fe-containing component in the initial stages. This must be converted into **4** or **5** and the dark, unidentified species seen in the room temperature studies. $HCo(CO)_4$ is initially formed, probably stoichiometrically, and then mainly undergoes conversion into H_2 and recycled $Co_2(CO)_8$. We also noticed another unidentified carbonyl-containing component of the reaction mixture which showed ions in the mass spectrum from $m/e \approx 637$ downwards. These aspects of the reaction system are being further investigated. The new compound **5** is the most striking product.

Characterisation of 5. The infrared spectrum shows a carbonyl stretching region which is similar in position and intensity of bands to that for [μ-$Ge\{Co(CO)_4\}Me]Co_2(CO)_7$ (**4**) [5,6], apart from the absence of a μ-CO mode. The mass spectrum shows very weak peaks for the parent ion, and the loss of CO from this, with loss of $Co(CO)_n$ as the major fragmentation process. The proton shift of **5** is very similar to those for **4** [5] and **6**. The compound readily gave single crystals, allowing determination of the molecular structure.

The structure, shown in Fig. 1, may be described as corresponding to that of $Co_2(CO)_8$ with both μ-CO groups replaced by μ-Ge[$Co(CO)_4$]Me units. The molecule has crystallographically imposed *mm* symmetry; one mirror plane includes the Co–Co bond and the second passes through the two Ge atoms and bisects the Me and terminal $Co(CO)_4$ units, giving molecular C_{2v} symmetry. Both $Co(CO)_4$ groups are directed outwards and the methyl groups inwards; although two other isomers are possible, this one clearly minimises intramolecular interactions. The dihedral angle between the two $GeCo_2$ triangles with a common edge is 113°.

The Co–Co bond length has increased to 2.733 Å from 2.529 Å [7] in $Co_2(CO)_8$, and this seems to be a result of replacing both bridges since in [μ-$Ge\{Co(CO)_4\}Ph]Co_2(CO)_7$, with μ-CO and μ-GePh[$Co(CO)_4$], the Co–Co distance is scarcely increased [8], to 2.54 Å. A similar change is seen [2] in the case of $Ge_3Co_8(CO)_{26}$, for which the outer Co–Co length (substituents one μ-CO and one

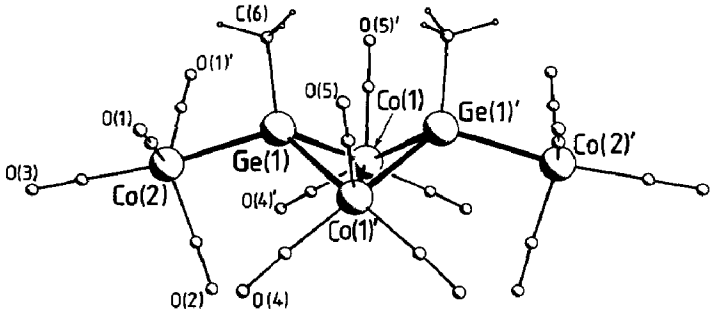

Fig. 1. A view of $[\mu\text{-Ge}\{Co(CO)_4\}Me]_2Co_2(CO)_6$. The central cobalt atoms lie on one crystallographic mirror plane, while the two germanium atoms and substituents lie on another.

μ-Ge[$Co_2(CO)_7$]) is 2.52 Å and the central one with two bridging germyl groups is 2.66 Å. In **5** the $GeCo_2$ triangles are symmetrical with Ge–Co 2.397 Å, in contrast to the slightly asymmetric triangles in $[\mu\text{-Ge}\{Co(CO)_4\}Ph]Co_2(CO)_7$ for which [8] Ge–Co are 2.375 and 2.392 Å. The external, terminal Ge–Co distances are the same in both species, at 2.455 Å, significantly longer than those in the core.

$[Fe(CO)_4GeMeH]_2$ (2) and $Co_2(CO)_8$. This reaction is much slower than that of **1**, requiring at least 15 days as shown by monitoring of the evolved gases. The H_2 content increased in the later part of the reaction, and significant amounts of $HCo(CO)_4$ were isolated. This implies the initial production of $HCo(CO)_4$, whose decay accounts for the continuing slower, H_2 evolution. The basic path is probably as shown in eq. 6.

$$\underset{(2)}{[Fe(CO)_4GeMeH]_2} + 2Co_2(CO)_8 \rightarrow \underset{(6)}{[\mu\text{-Ge}\{Co(CO)_4\}Me]_2Fe_2(CO)_7} + 2HCo(CO)_4 + CO \quad (6)$$

With the long reaction time, most of the $HCo(CO)_4$, reacts to form H_2 and $Co_2(CO)_8$. The removal of the gases also enhances the formation of $Co_4(CO)_{12}$, which causes difficulties in separation, and low recovery of **6**. In the sealed tube experiments this last reaction was suppressed, and a high yield of **6** resulted. The best procedure thus involves reaction in a sealed tube for 2–3 weeks. Allowing for handling losses, the conversion of **2** into **6** was quantitative.

Characterisation of 6. The carbonyl stretching region in the IR spectrum is quite similar to that of **5**, but showed a μ-CO mode at 1845 cm^{-1}, indicating a $Fe_2(\mu\text{-CO})$ unit. The mass spectrum showed a weak parent ion, and loss of 15CO, but the dominant fragmentation was loss of $Co(CO)_4$ from the parent. Single crystals were obtained, allowing determination of the molecular structure of **6** (Fig. 2).

The structure is shown in Fig. 2. The Ge–H bonds of **2** have been replaced by Ge–$Co(CO)_4$ bonds, and the four-membered FGeFeGe ring has been closed by formation of an Fe–Fe bond, accompanied by a bridging CO, just as was observed [3,4] for $[Fe(CO)_4GeH_2]_2$, eq. 2. The structure can be alternatively described as that of $Fe_2(CO)_9$ with two of the μ-CO groups replaced by μ-Ge[$Co(CO)_4$]Me units. The molecule lies on a crystallographic mirror plane which contains the Fe–(μ-CO)–Fe unit. The two $Co(CO)_4$ groups are directed outwards and the methyl groups

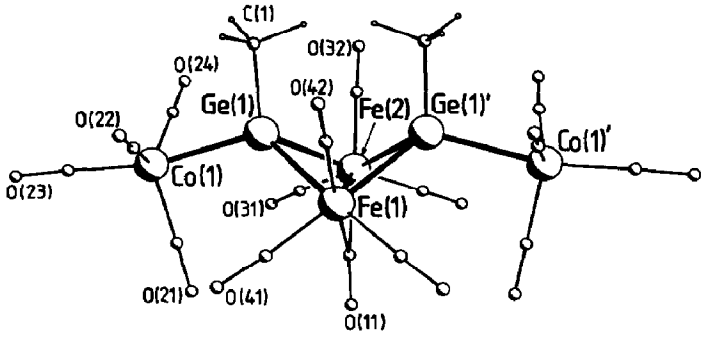

Fig. 2. A view of $[\mu\text{-Ge}\{Co(CO)_4\}Me]_2Fe_2(CO)_7$. A crystallographic mirror plane incorporates the two iron atoms and the bridging carbonyl group.

inwards, as was observed above for **5**. The dihedral angle across the Fe–Fe bond is 111.9°.

The Fe–Fe bond (2.691(5) Å) is markedly longer than in $Fe_2(CO)_9$, 2.523(1) Å, [9], and is comparable with that [10] in $(Ph_2Ge)_2Fe_2(CO)_7$ (2.666(3) Å). A similar value (2.678 Å) was found [2] for $Ge_2Fe_2Co_4(CO)_{21}$. In contrast to those in these two related molecules, the $GeFe_2$ and $Fe_2(\mu\text{-CO})$ triangles of **6** are symmetric. The external Ge–Co distance (2.455(3) Å) is identical to that in **5**.

Discussion

$[Fe(CO)_4(GeMeH_2)_2]$ (1) plus $Co_2(CO)_8$. The main isolated product from the reactions in solution is **5**, which incorporates both methylgermanium groups from **1**, while the product containing only one such group, $[\mu\text{-Ge}\{Co(CO)_4\}Me]Co_2(CO)_7$ (**4**) was present in only about a fifth of the amount of **5**.

The smooth formation of **5**, as in eq. 4, is reasonably understood as a result of the close proximity of the two methylgermyl groups in the *cis*-octahedral configuration of the iron compound. As for the earlier reactions of GeH_3 groups bonded to methylsilyl residues [11], the iron carbonyl group acts as a template to offer to the cobalt carbonyl the two germyl groups in close proximity. Extrusion of the $Fe(CO)_4$ unit must mainly occur late in the reaction, otherwise a greater proportion of the mono-germanium **4** would be produced. The reaction of $Co_2(CO)_8$ with $[Fe(CO)_4(GeH_3)_2]$ apparently proceeds via a similar path, but equal amounts of the mono-germanium $Ge[Co_2(CO)_7]_2$ and the di-germanium $Ge_2Co_6(CO)_{20}$ suggests earlier cleavage of Ge–Fe is more probable in the GeH_3 species, perhaps reflecting the bulkier products.

The unidentified black fraction was a mixture whose main components could not be separated or characterised. The results of reactions in the absence of solvent suggest the formation of a compound **3**, which could be formulated as the trigonal bipyramidal $(MeGe)_2FeCo_2(CO)_8$. This would agree with the IR spectra, and would be a logical product from a reaction in which both GeH_2 groups add to the same $Co_2(CO)_8$ molecule. Formation of **5** from **3** involves replacement of the $Fe(CO)_4$ group by a $Co(CO)_4$ unit, possibly by reaction with $HCo(CO)_4$. Some $Fe(CO)_5$ was found, but no evidence for other iron or iron–cobalt carbonyls. There must be a further iron-rich product: the $m/e \approx 637$ species in the low temperature reaction

and the dark, soluble, mixed fraction in the room temperature reaction are possible candidates. These aspects of the reaction need further study.

$[Fe(CO)_4GeMeH]_2$ (2) and $Co_2(CO)_8$. In contrast to the reaction with **1**, the product from **2** with $Co_2(CO)_8$ is formed quantitatively under sealed tube conditions, retains the Ge–Ge bonds, and has the Ge–H bonds replaced by Ge–$Co(CO)_4$ bonds. The reaction is similar to that in eq. 2, with a $Fe(\mu\text{-}CO)(\mu\text{-}GeZ_2)_2Fe$ unit formed in place of the four-membered FeGeFeGe ring of **2**. In the case of reaction 2, an intermediate product retaining the four-membered ring was isolated [2,3], and this reaction (eq. 6) may follow a similar course, proceeding via the four-membered FeGeFeGe ring with the formation of the Fe–Fe bond as the final step. However, as the later stages of the gas evolution were very slow, a separate decarbonylation stage [2] was not detected in this reaction.

Structural studies. No previous crystal structures have been reported for $Co_2(CO)_8$ species disubstituted by group 14 ligands, though $(Me_2Ge)_2Co_2(CO)_6$ and related species with bridging group 14 or 15 atoms have been studied by ^1H NMR spectroscopy [12,13]. Similarly, there are few structurally characterised substituted $Fe_2(CO)_9$ species, only $(Ph_2Ge)_2Fe_2(CO)_7$ and $(Me_2Ge)_3Fe_2(CO)_6$ being available for direct comparison [10].

The compounds **5** and **6** are isoelectronic species and the similarity between the two structures is striking. The extra carbonyl across the central M–M bond in **6** compared with **5** has little effect on the geometry of the rest of the molecule, the Fe–Fe bond in **6** being marginally shorter than the Co–Co bond in **5**, with the Ge–Fe bonds correspondingly slightly longer than Ge–Co bonds. Comparison with the respective dinuclear binary carbonyls shows the increases in the length of the metal–metal bond on replacement of the two μ-CO by μ-$MeGeCo(CO)_4$ units are almost identical: 0.23 Å for Fe–Fe and 0.213 Å for Co–Co. The outer Ge–Co and Ge–C bond lengths are the same in both compounds, with values similar to those in less sterically crowded species.

Compared with that of $Co_2(CO)_8$, the structures of **5** and **6** display remarkably small dihedral angles between the triangles formed by the M–M bond and the bridging atoms. In $Co_2(CO)_8$ the dihedral angle involving the bridging carbonyls is 130° [7], but replacing these with the ostensibly bulkier group μ-Ge{$Co(CO)_4$}Me to give **5** leads to a closing of the dihedral angle to 113°. The $Fe_2(CO)_9$ derivatives **6** shows a similar effect, with a Ge(1)Fe(1)Fe(2)/Ge(1)'Fe(1)Fe(2) angle of 112°, significantly less than the 120° for the corresponding angle in the parent carbonyl; this value is virtually indistinguishable from the 111° found for [μ-Ge{$Co_2(CO)_7$}]$_2Fe_2(CO)_7$ [2,3]. What is noticeable in all of these compounds is that the Ge...Ge non-bonded distance is essentially constant at 3.30 Å, which suggests that the dihedral angles adjust to maintain an optimum distance between the bridging atoms; although germanium is a bigger atom than carbon, the longer Ge–M bonds compared to C–M bonds allow a smaller dihedral angle across a M–M bond without giving excessive Ge...Ge interactions. In $(\mu\text{-}GePh_2)_2Fe_2(CO)_7$ the dihedral angle between the $GeFe_2$ planes was 126° with a longer Ge...Ge distance of 3.65 Å, but for this example the interaction of the Ph groups on the Ge atoms is likely to be dominant [10]. In a number of species containing (μ-GeR_2)$Co_2(\mu\text{-}CO)$ groups a fairly constant value for the Ge...C distance of 2.77 Å was noted despite quite different values for the dihedral angles [14]. It has been shown in other systems involving butterfly clusters that quite large variation of the

dihedral angles involves small energy changes [15], so that optimisation of non-bonded interactions will determine the precise conformation in each example.

It has been shown by ^{1}H NMR studies on $(\mu\text{-}GeMe_2)_2Co_2(CO)_6$ and related species that at room temperature there is fluxional averaging of the *syn* and *anti* methyl groups, but that at low temperatures the inequivalence of the methyls arising from the non-planarity of the bridging groups can be frozen out [12,13]. For **5** and **6** only one sharp Me signal was apparent in the ^{1}H NMR spectra, suggesting that the structures found in the solid state are maintained in solution; there was no evidence for the alternative isomers with either one or both methyl groups in the *anti* conformation. This is not unexpected in view of the different steric requirements of the two groups on the Ge atoms.

A striking feature common to the mass spectra of **5** and **6** is the facile loss of one $Co(CO)_4$ group from these molecules. This was not seen for **4** [4,5] nor for its Ph analogue [8], nor was the terminal $Co(CO)_4$ readily lost from the closed cluster $[(CO)_4Co]GeCo_3(CO)_9$ [16]. Thus the loss does not result from the presence of the Ge–$Co(CO)_4$ linkage, but must reflect the steric pressures in **5** and **6**. This suggests, in turn, that **5** and **6** will be of interest as starting molecules for the synthesis of new clusters, especially by decarbonylation reactions; in particular **5** undergoes CO elimination to give the *closo*-cluster $(MeGe)_2Co_4(CO)_{11}$ [17]. Further details will be the subject of future publications.

Experimental

Compounds were handled on conventional vacuum lines or under dry N_2 in Schlenk lines and glove boxes. Preliminary reactions without solvent were carried out on a conventional vacuum line. Reactions in hexane were carried out in tubes of ca. 50 ml volume fitted with greaseless taps. Gases incondensable in liquid nitrogen were measured at intervals with a Toepler pump and gas burette. Approximate compositions, on the assumption that only H_2 and CO were formed, were derived from measurements of average molecular weight. The total gas measurement is accurate to 1–2%, but the composition is subject to an uncertainty of 5–20%, depending on the quantity of gas formed. Mixed solid fractions were examined by mass spectroscopy (sample handling under argon) with the inlet at different temperatures, allowing partial separation and fairly confident identification of the fragment ions arising from each species by variations in intensities with temperature. For the solution reactions, the hexane was condensed off and examined for any volatile by-products by infrared spectroscopy. The main product mixtures were involatile, and these were worked up by extraction and recrystallisation. The preparations of the iron carbonyl starting materials **1** and **2** have been described previously [4].

$[Fe(CO)_4(GeMeH_2)_2]$ (1) plus $Co_2(CO)_8$

(a) Direct reaction of solids at 0°C. [18].* **1** (128 mg, 0.37 mmol) was condensed on to $Co_2(CO)_8$ (421 mg, 1.23 mmol) and the mixture kept at 0°C. Gases

* Reference number with asterisk indicates a note in the list of references.

were removed at intervals by Toepler pump, through a trap kept at −196 °C. 0.40 mmol was collected in 24 h rising to 0.81 mmol total after 9 d, when the reaction was stopped. The H_2/CO ratio was 1/4.5; thus about 20% of the hydrogen content of **1** was recovered as H_2.The cold-trap contained $HCo(CO)_4$ (110 mg, 0.64 mmol) and a trace of $Fe(CO)_5$. Unchanged **1** and $Co_2(CO)_8$ were removed by pumping for 2 d. A brown sublimate free from starting material was then obtained by pumping at room temperature for a further week. The mass spectrum of this material, examined at inlet temperatures of 30, 60, and 100 °C, showed the presence of $Co_4(CO)_{12}$ (ca. 20% of ion current), $[\mu\text{-Ge}\{Co(CO)_4\}Me]Co_2(CO)_7$ (**4**) (ca. 75% of ion current) and a small amount of a third species. From the residual solid, a modest amount of further sublimate was obtained at 40 °C and its ^1H NMR spectrum showed signals at δ 2.0 (**4**), 1.29, 0.9 and 0.83 in the ratio 2/6/1/1.

The non-sublimable solid was then extracted with cyclohexane, and mass spectra of the recovered solid were recorded at 20 and 80 °C. The spectrum at 20 °C was clean, and showed a strong parent ion family, with an isotope pattern appropriate for 2Ge, at $m/e = 568–580$, corresponding to $Me_2Ge_2Co_2Fe(CO)_8^+$. The series $[P - nCO]^+$ was prominent with n = 1(m), 2(w), 3(m), 4(vs), 5(s), 6(s), 7(s), and 8(vs). There were weak families corresponding to the additional loss of one Me for n = 1 and 6. In addition, an envelope at $m/e = 328–341$ showed a different pattern of peak heights with a smooth profile corresponding to the concurrent losses of Me and Me + H to give $CH_xGe_2Co_2Fe^+$ for x = 3 and 2. The $Ge_2Co_2Fe^+$ ion was very strong, and strong peaks at m/e = 56 and 59 established the presence of Fe and Co. All other ions were very weak, and there were also present very weak ions from $[\mu\text{-Ge}\{Co(CO)_4\}Me]Co_2(CO)_7$. The mass spectrum of the hexane extract at 80 °C showed a stronger spectrum of this $Me_2Ge_2Co_2Fe(CO)_8$ species, together with the major ions [17] from $(MeGe)_2Co_4(CO)_{11}$. This latter compound was the major component in a CH_2Cl_2 extract of the product mixture.

In a similar experiment, but with work-up without the prolonged pumping/sublimation steps, the total solid sample gave a mass spectrum at inlet temperatures of 60 and 80 °C, with a weak parent ion envelope centred at m/e = 804, corresponding to the compound $[\mu\text{-Ge}\{Co(CO)_4\}Me]_2Co_2(CO)_6$ (**5**), characterised below. From this, five fragment ion envelopes corresponding to losses of n CO and of $Co(CO)_n$ were seen down to m/e = ca. 635. For the following CO losses the envelopes were broader, and the two wings varied in relative intensities at the two temperatures, indicating a second species with highest mass ion around 637. Further broadening and variability marked the presence of $Me_2Ge_2Co_2Fe(CO)_8$ from ca. m/e = 570 downwards. Other significant though minor intensity low mass fragments were Fe, GeGe, GeCo, MeGeFe, and MeGeCo as well as iron and cobalt (hydride) carbonyl series. The major features of the IR spectrum of the most hexane-soluble fraction were bands at 2042m, 2015s,br, 1880w, 1855w cm^{-1}.

(b) In solution at room temperature. In hexane, **1** (510 mg, 1.46 mmol) and $Co_2(CO)_8$ (900 mg, 2.62 mmol) reacted rapidly, the colour changing from wine-red to red-brown, and a small amount of yellow precipitate redissolved on shaking. Gas evolution was very rapid initially, with 3.94 mmol formed in the first 15 min, rising to 4.31 mmol in 45 min, and then increasing linearly and slowly to 5.12 mmol after 17 h, when the reaction was stopped. The H_2/CO ratio stayed approximately constant at 1/1.35, and 78 ± 10% of the hydrogen content of **1** was recovered as H_2. The solvent fraction contained $Fe(CO)_5$ and a minor amount of $HCo(CO)_4$, but

these could not be separated for quantitative determination. There was no unchanged **1** or any $MeGeH_3$.

The product mixture was readily soluble in hexane, and recrystallisation yielded a new orange product, shown below to be $[\mu\text{-Ge}\{Co(CO)_4\}Me]_2Co_2(CO)_6$ (**5**) (650 mg, 0.70 mmol, 48%); $[\mu\text{-Ge}\{Co(CO)_4\}Me]Co_2(CO)_7$ (**4**) (50 mg, 0.08 mmol, 12%), IR and mass spectrum agreeing with published observations [5,6]; a trace of $Co_4(CO)_{12}$; and a black fraction (290 mg) with ν(CO) 2095w, 2087w, 2078vw, 2072mw, 2053w, 2039vvs, 2029mw, 2018vvs, 2005w, 1859w cm^{-1}, where the 2072, 2039, 2018, and 1859 bands indicate one or more new products and both **4** and **5** are present in minor amounts.

In a reaction with a higher proportion of $Co_2(CO)_8$ continued for 50 h, **1** (810 mg, 2.34 mmol) and $Co_2(CO)_8$ (2.21 g, 6.4 mmol) formed 10.1 mmol gas (H_2/CO 1/1.65), with 75% of the total gas evolution occurring in the first 15 min and only 6% in the final 33 h allowed for this reaction. The solvent fraction contained $Fe(CO)_5$ (ca. 0.2 mmol) and a small undetermined amount of $HCo(CO)_4$. After work-up, removal of unchanged $Co_2(CO)_8$ and recrystallisation there were recovered **5** (690 mg, 0.85 mmol, 36%); **4** (160 mg, 0.16 mmol, 7%); $Co_4(CO)_{12}$ (16 mg, 0.03 mmol, 1%); and the black fraction (320 mg).

The mass spectrum of **5** showed a very weak parent ion, and four weak ions formed by CO losses. The dominant feature was loss of $Co(CO)_4$ giving a series of 10 ions $Me_2Ge_2Co_3(CO)_x^+$ for $x = 9$ to 0 together with five minor $Me_aGeCo(CO)_b^+$ fragments ($a = 2, 1$; $b = 2, 1, 0$). The CO stretching region of the infrared spectrum showed (cm^{-1}): 2097w, 2087s, 2067m, 2042w, 2039m, 2029m, 2017s, 2002w, 1989w, 1970w. The ^1H NMR spectrum in $CDCl_3$ gave a single peak at δ 2.0. Full characterisation was provided by an X-ray crystal structure determination (see below).

$[Fe(CO)_4(GeH_3)_2]$ plus $Co_2(CO)_8$. Analogous reactions between $[Fe(CO)_4(GeH_3)_2]$ and $Co_2(CO)_8$ in hexane for 20 to 40 h on a 0.5 mmol scale and in ratios 1/3–4, gave a mixture containing $Ge[Co_2(CO)_7]_2$ and $Ge_2Co_6(CO)_{20}$ in similar proportions, corresponding to about 30% recovery of germanium. Further material was recovered as hexane-soluble and hexane-insoluble dark fractions. The soluble fraction was distinguished by very strong IR bands at 2039 and 2019 cm^{-1}, as in the methyl system above. The insoluble fraction showed a poorly resolved, IR spectrum with bands at 2098w, 2037sh, 2019vs, 1997s, 1990–50v br, 1926sh, 1918s, 1907s, 1844w, and 1832w cm^{-1}.

$[Fe(CO)_4GeMeH]_2$ (2) plus $Co_2(CO)_8$. Complex **2** (190 mg, 0.38 mmol) and $Co_2(CO)_8$ (130 mg, 0.37 mmol) reacted slowly in hexane. One third of the total gas evolution occurred in the first 3 h (composition 40% H_2) but slow evolution continued for 10 d. The reaction was stopped at this point, with a total gas evolution of 0.32 mmol, (composition 44% H_2). $HCo(CO)_4$ (0.07 mmol, 10%) was fractionated from the solvent, and a hexane-soluble black solid fraction was recovered. Unchanged $Co_2(CO)_8$ was sublimed out, leaving a mixture of $Co_4(CO)_{12}$ and a new species with a prominent IR band at 2089 cm^{-1}, and shown below to be **6**. It took several recrystallisations, and much sacrifice of material, to substantially reduce the proportion of $Co_4(CO)_{12}$ and so give a pure sample of **6**. A second experiment under the same conditions but using a deficiency of $Co_2(CO)_8$ gave similar results.

When the reaction was carried out in a sealed tube in the dark, a sample of **2** (321 mg, 0.63 mmol) shaken in pentane with $Co_2(CO)_8$ (228 mg, 0.67 mmol) formed light

orange crystals, mixed with a few black ones, within a week. No further changes could be detected during the next 4 weeks and the reaction was stopped. There were isolated: gases (1.30 mmol; 41% H_2), $HCo(CO)_4$ in the hexane which was not separated, and an involatile orange fraction. This was separated into two by careful washing with pentane to give a more soluble fraction (70 mg) consisting of $Co_4(CO)_{12}$ plus some $[Ge\{Co(CO)_4\}Me]_2Fe_2(CO)_7$, and a less soluble fraction which was pure $[Ge\{Co(CO)_4\}Me]_2Fe_2(CO)_7$ (**6**) (391 mg, 0.47 mmol, 76%). In another experiment the sample of **2** contained a small amount of **1** (391 mg, 0.76 mmol calculated as **2**) showed similar changes when shaken with $Co_2(CO)_8$ (291 mg, 0.85 mmol) for 4 weeks. There were isolated: gases (1.67 mmol; 40% H_2); $HCo(CO)_4$ in the hexane which was not separated; an orange fraction slightly soluble in pentane, shown below to be $[Ge\{Co(CO)_4\}Me]_2Fe_2(CO)_7$ (**6**) (550 mg, 0.67 mmol, 88%); now only a trace of $Co_4(CO)_{12}$; and black crystals (38 mg), soluble in CH_2Cl_2. The black crystals were found to be $(MeGe)_2Co_4(CO)_{11}$ (0.054 mmol) by comparison of the spectroscopic properties [16]. On the assumption that this was formed directly from the content of **1** in the sample of **2**, the yield of 6 from **2** becomes about 95%.

The product **6** is light orange, poorly soluble in pentane or hexane but readily soluble in CH_2Cl_2. The solid is stable for short periods in air but in solution decomposes rapidly. The solution and solid are stable indefinitely at 4°C under N_2. On electron probe analysis of **6** gave a ratio of Ge/Co/Fe = 1.03/1.0/1.0. Three successive mass spectra scans gave, as heaviest ions, (i) $[P - Co(CO)_4]^+$, (ii) P^+ followed by $[P - Co(CO)_4]^+$ and (iii) P^+ followed by 3 CO losses, then by $[P - Co(CO)_4]^+$. In each case, $[P - Co(CO)_4]^+$ was followed by further loss of 11 consecutive CO groups. This suggests that the sample was heating up steadily, allowing weaker ions to be seen in progression.

The IR spectrum of **6**, in CH_2Cl_2/pentane, showed carbonyl stretching bands at (cm^{-1}): 2090ms, 2068w, 2052m, 2030vs, 2013s, 1995s, 1844w: and in a CsI disc: 2086s, 2069sh, 2048m, 2030s, 2016s, 2000sh, 1992vs, 1974s, 1945sh, 1845s. A ^1H NMR spectrum in $CDCl_3$ gave a single peak at δ 2.04. Further characterisation was by an X-ray structure determination.

X-ray crystallography. Suitable crystals of **5** and **6** were grown from CH_2Cl_2/hexane. Preliminary precession photography showed each formed a centred orthorhombic lattice with systematic absences appropriate for *Cmcm*, $Cmc2_1$ or *Ama*2, with the final assignment based on E-statistics and on the successful refinements.

Table 1

Final positional parameters for $[\mu\text{-}Ge\{Co(CO)_4\}Me]_2Co_2(CO)_6$

Atom	*x*	*y*	*z*	Atom	*x*	*y*	*z*
Ge(1)	0.0	0.1668(1)	0.1601(1)	C(3)	0.0	0.2549(8)	−0.0655(7)
Co(1)	0.1198(1)	0.2524(1)	0.25	O(3)	0.0	0.2739(8)	−0.1237(5)
Co(2)	0.0	0.2267(1)	0.0324(1)	C(4)	0.1901(6)	0.3256(5)	0.1796(3)
C(1)	0.1366(7)	0.1584(6)	0.0353(4)	O(4)	0.2433(5)	0.3716(5)	0.1381(3)
O(1)	0.2258(5)	0.1178(5)	0.0371(3)	C(5)	0.2101(8)	0.1387(7)	0.25
C(2)	0.0	0.3632(8)	0.0615(6)	O(6)	0.2689(7)	0.0650(6)	0.25
O(2)	0.0	0.4492(6)	0.0767(5)	C(6)	0.0	0.0119(6)	0.1518(5)

Table 2

Final positional parameters for $[\mu\text{-Ge}\{Co(CO)_4\}Me]_2Fe_2(CO)_7$

Atom	x	y	z	Atom	x	y	z
Ge(1)	0.0903(1)	0.2244(1)	0.5618(1)	C(24)	0.211(1)	0.326(2)	0.479(2)
C(1)	0.093(1)	0.138(2)	0.418(2)	O(24)	0.2080(9)	0.377(1)	0.391(2)
Co(1)	0.2164(1)	0.2543(2)	0.6136(3)	C(11)	0.000	0.336(2)	0.771(2)
Fe(1)	0.000	0.3628(3)	0.5869(4)	O(11)	0.000	0.385(2)	0.855(2)
Fe(2)	0.000	0.1819(3)	0.7142(4)	C(31)	−0.0733(9)	0.457(1)	0.601(2)
C(21)	0.195(1)	0.328(2)	0.749(2)	O(31)	−0.1142(8)	0.523(1)	0.609(1)
O(21)	0.1815(9)	0.375(1)	0.837(1)	C(32)	0.000	0.359(4)	0.427(4)
C(22)	0.211(1)	0.114(1)	0.632(2)	O(32)	0.00	0.368(2)	0.323(2)
O(22)	0.210(1)	0.023(1)	0.640(1)	C(41)	−0.071(1)	0.159(2)	0.821(2)
C(23)	0.313(1)	0.260(2)	0.622(2)	O(41)	−0.1159(8)	0.135(1)	0.887(1)
O(23)	0.375(1)	0.267(1)	0.634(1)	C(42)	0.000	0.049(3)	0.642(3)
O(42)	0.00	−0.035(2)	0.602(2)				

Cell parameters were obtained on an Enraf–Nonius CAD4 (for **5**) and a Nicolet XRD P3 (for **6**) diffractometer using monochromated Mo-K_α X-rays.

Crystal data for **5**: $C_{16}H_6Co_4Ge_2O_{14}$, $M = 803.07$, orthorhombic, space group *Cmcm*, *a* 11.402(4), *b* 12.698(3), *c* 18.285(8) Å, *U* 2647(1) Å^3. $D_c = 2.01$ g cm^{-3} for $Z = 4$. F(000) 1544, μ(Mo-K_α) 56 cm^{-1}, *T* 292 K, orange crystal 0.60 × 0.65 × 0.25 mm. Intensity data in the range $4 < 2\theta < 54°$ were collected using a θ–2θ scan. Empirical absorption corrections were made (transmission factors 0.99 max., 0.56 min.) A total of 1392 unique reflections were recorded and those 1013 for which $I > 2\sigma(I)$ were used in all calculations.

Table 3

Bond lengths and angles for $[\mu\text{-Ge}\{Co(CO)_4Me]_2Co_2(CO)_6$

Bond lengths (Å)		Bond angles (°)	
Ge(1)–Co(1)	2.398(1)	Co(1)–Ge(1)–Co(2)	120.8(1)
Ge(1)–Co(2)	2.454(2)	Co(1)–Ge(1)–C(6)	120.3(2)
Ge(1)–C(6)	1.973(8)	Co(1)–Ge(1)–Co(1)	69.5(1)
Co(1)–Co(1)′	2.733(2)	Co(2)–Ge(1)–C(6)	103.6(3)
Co(1)–C(4)	1.778(6)	Ge(1)–Co(1)–C(4)	89.8(2)
Co(1)–C(5)	1.773(9)	Ge(1)–Co(1)–C(5)	87.8(2)
Co(2)–C(1)	1.783(7)	C(4)–Co(1)–C(5)	99.4(3)
Co(2)–C(2)	1.81(1)	Ge(1)–Co(2)–C(1)	79.7(2)
Co(2)–C(3)	1.83(1)	Ge(1)–Co(2)–C(2)	91.0(3)
C(1)–O(1)	1.140(8)	Ge(1)–Co(2)–C(3)	173.3(3)
C(2)–O(2)	1.13(1)	C(1)–Co(2)–C(2)	117.1(2)
C(3)–O(3)	1.09(1)	C(1)–Co(2)–C(3)	97.1(3)
C(4)–O(4)	1.133(7)	C(2)–Co(2)–C(3)	95.7(4)
C(5)–O(5)	1.15(1)	Co(2)–C(1)–O(1)	177.8(7)
		Co(2)–C(2)–O(2)	177(1)
		Co(2)–C(3)–O(3)	178(1)
		Co(1)–C(4)–O(4)	174.2(7)
		Co(1)–C(5)–O(5)	179.9(2)
Dihedral angle			
Ge(1)Co(1)Co(1)′/Ge(1)′Co(1)Co(1)′		113.1°	

Table 4

Bond lengths and angles for $[\mu\text{-Ge}\{Co(CO)_4\}Me]_2Fe_2(CO)_7$

Bond lengths (Å)			
Ge(1)–C(1)	1.95(2)	Fe(2)–C(11)	2.05(3)
Ge(1)–Co(1)	2.455(3)	Fe(2)–C(41)	1.8(2)
Ge(1)–Fe(1)	2.444(3)	Fe(2)–C(42)	1.86(4)
Ge(1)–Fe(2)	2.459(3)	C(21)–O(21)	1.17(2)
Co(1)–C(21)	1.83(2)	C(22)–O(22)	1.15(2)
Co(1)–C(22)	1.79(2)	C(23)–O(23)	1.17(3)
Co(1)–C(23)	1.81(2)	C(24)–O(2)	1.18(3)
Co(1)–C(24)	1.76(2)	C(11)–O(11)	1.12(3)
Fe(1)–Fe(2)	2.691(5)	C(31)–O(31)	1.13(2)
Fe(1)–C(11)	2.09(2)	C(32)–O(32)	1.17(5)
Fe(1)–C(31)	1.82(2)	C(41)–O(41)	1.16(3)
Fe(1)–C(32)	1.80(5)	C(42)–O(42)	1.15(4)
Bond angles (°)			
C(1)–Ge(1)–Co(1)	105.1(6)	C(11)–Fe(1)–C(32)	169(2)
C(1)–Ge(1)–Fe(1)	120.7(6)	C(31)–Fe(1)–C(32)	96(1)
C(1)–Ge(1)–Fe(2)	117.9(6)	Ge(1)–Fe(2)–Fe(1)	56.4(1)
Co(1)–Ge(1)–Fe(1)	121.7(1)	Ge(1)–Fe(2)–C(11)	90.5(5)
Co(1)–Ge(1)–Fe(2)	121.8(1)	Ge(1)–Fe(2)–C(41)	175.4(7)
Fe(1)–Ge(1)–Fe(2)	66.6(1)	Ge(1)–Fe(2)–C(42)	83.9(8)
Ge(1)–Co(1)–C(21)	93.5(7)	Fe(1)–Fe(2)–C(11)	50.2(7)
Ge(1)–Co(1)–C(22)	79.4(6)	Fe(1)–Fe(2)–C(41)	119.3(7)
Ge(1)–Co(1)–C(23)	167.4(7)	Fe(1)–Fe(2)–C(42)	122(1)
Ge(1)–Co(1)–C(24)	79.5(6)	C(11)–Fe(2)–C(41)	87.3(8)
C(21)–Co(1)–C(22)	113.2(9)	C(11)–Fe(2)–C(42)	172(1)
C(21)–Co(1)–C(23)	99.1(9)	C(41)–Fe(2)–C(42)	98(1)
C(21)–Co(1)–C(24)	115.9(8)	Co(1)–C(21)–O(21)	179(2)
C(22)–Co(1)–C(23)	95.4(9)	Co(1)–C(22)–O(22)	176(2)
C(22)–Co(1)–C(24)	127.2(9)	Co(1)–C(23)–O(23)	176(2)
C(23)–Co(1)–C(24)	94(1)	Co(1)–C(24)–O(24)	177(2)
Ge(1)–Fe(1)–Fe(2)	57.0(1)	Fe(1)–C(11)–Fe(2)	81.1(9)
Ge(1)–Fe(1)–C(11)	89.9(5)	Fe(1)–C(11)–O(11)	137(2)
Ge(1)–Fe(1)–C(31)	174.8(6)	Fe(2)–C(11)–O(11)	141(2)
Ge(1)–Fe(1)–C(32)	82(1)	Fe(1)–C(31)–O(31)	173(2)
Fe(2)–Fe(1)–C(11)	48.7(7)	Fe(1)–C(32)–O(32)	172(4)
Fe(20–Fe(1)–C(31)	120.6(5)	Fe(2)–C(41)–O(41)	174(2)
Fe(2)–Fe(1)–C(32)	120(2)	Fe(2)–C(42)–O(42)	176(3)
C(11)–Fe(1)–C(31)	91.1(7)		
Dihedral angle			
Ge(1)Fe(1)Fe(2)/Ge(1)′Fe(1)Fe(2)		111.9°	

The structure was solved by direct methods and routinely developed. In the final cycles of full-matrix least-squares refinement all atoms were assigned anisotropic temperature factors. Hydrogen atoms were not included. The refinement converged with $R = 0.0387$, $R_w = 0.0401$ where $w = [\sigma^2(F) + 0.0008F^2]^{-1}$, with no final shifts greater than 0.01σ, and with no residual electron density > 0.6 e Å^{-3}.

Crystal data for **6**: $C_{17}H_6Co_2Fe_2Ge_2O_{15}$, $M = 824.97$, orthorhombic, space group $Cmc2_1$, a 18.676(3), b 12.614(2), c 11.209(2) Å, U 2640.6(6) Å^3. $D_c = 2.07$ g cm^{-3} for $Z = 4$. $F(000)$ 1592, μ(Mo-K_α) 46 cm^{-1}, T 292 K, orange crystal $0.46 \times 0.46 \times 0.07$ mm. Intensity data in the range $4 < 2\theta < 50°$ were collected

using Wycoff scans. The data were corrected for Lorentz, polarisation and absorption effects (transmission factors 0.78 max., 0.25 min.). A total of 1189 unique reflections were recorded and those 919 for which $I > 3\sigma(I)$ were used in all calculations.

The structure was solved by direct methods and routinely developed. In the final cycles of full-matrix least-squares refinement metal atoms were assigned anisotropic temperature factors, while other atoms were treated isotropically. The hydrogen atoms were included in calculated positions with a common isotropic temperature factor.The refinement converged with $R = 0.0684$, $R_w = 0.0694$ where $w = [\sigma^2(F) + 0.003F^2]^{-1}$, with no final shifts greater than 0.1σ. A final difference map showed three residual peaks 2–3 e $Å^{-3}$ in height adjacent to the metal atoms; these are probably artifacts arising from an imprecise absorption correction for a very thin plate crystal, but a partial disorder of the metal skeleton cannot be discounted.

For both structures calculations were performed using the SHELX86 or SHELX76 programs [19]. Final positional parameters are listed in Table 1 and 2, selected bond parameters in Tables 3 and 4 while the structures are illustrated in Figures 1 and 2 for **5** and **6**, respectively.

Acknowledgements

We thank Dr. Ward T. Robinson, University of Canterbury, and Dr. Cliff Rickard, University of Auckland, for collection of X-ray intensity data. Grateful acknowledgement is made to the New Zealand Universities' Grants Committee, and to the donors of the Petroleum Research Fund, administered by the ACS, for financial support.

References

1 J.A. Christie, D.N. Duffy, K.M. Mackay, and B.K. Nicholson, J. Organomet. Chem., 226 (1982) 165.
2 S.G. Anema, K.M. Mackay, L.C. McLeod, B.K. Nicholson, and J. Whittaker, Angew. Chem., Int. Ed. Engl., 25 (1986) 759.
3 S.G. Anema, J.A. Audett, K.M. Mackay, and B.K. Nicholson, J. Chem. Soc., Dalton Trans., (1988) 2629.
4 A. Bonny and K.M. Mackay, J. Chem. Soc., Dalton Trans., (1978) 506, 1569; J.A. Audett and K.M. Mackay, J. Chem. Soc., Dalton Trans., (1988) 2635.
5 R.F. Gerlach, B.W.L. Graham and K.M. Mackay, J. Organomet. Chem., 182 (1979) 285.
6 G. Etzrodt and G. Schmid, J. Organomet. Chem., 169 (1979) 259.
7 G. Sumner, H. Klug, and L. Alexander, Acta Cryst., 17 (1964) 732; P.C. Leung and P. Coppens, Acta Cryst., B, 39 (1983) 535.
8 R. Ball, M.J. Bennett, E.H. Brookes, W.A.G. Graham, J. Hoyano, and S.H. Illingworth, Chem. Comm., (1970) 592.
9 F.A. Cotton and J.M. Troup, J. Chem. Soc., Dalton Trans., (1974) 800.
10 M. Elder, Inorg. Chem., 8 (1969) 2703; M. Elder and D. Hall, ibid., 8 (1969) 1424.
11 S.P. Foster, K.-F. Leung, K.M. Mackay, and R.A. Thomson, Aust. J. Chem., 39 (1986) 1089.
12 R.D. Adams and F.A. Cotton, J. Am. Chem. Soc., 92 (1970) 5003.
13 R.D. Adams, F.A. Cotton, W.R. Cullen, D.L. Hunter, and L. Mihichuk, Inorg. Chem., 14 (1975) 1395.
14 R.F. Gerlach, K.M. Mackay, B.K. Nicholson and W.T. Robinson, J. Chem. Soc., Dalton Trans., (1981) 80.
15 M.I. Bruce and B.K. Nicholson, J. Organomet. Chem., 250 (1983) 627.
16 G. Schmid and G. Etzrodt, J. Organomet. Chem., 137 (1977) 361; G. Schmid, V. Batzel, and G. Etzrodt, ibid., 112 (1976) 345.

17 S.P. Foster, K.M. Mackay and B.K. Nicholson, J. Chem. Soc., Chem. Comm., (1982) 1156.
18 Preliminary experiments carried out by A Bonny, Waikato.
19 G.M. Sheldrick, SHELX76, Program for the Determination of X-ray Crystal Structures, University of Cambridge, 1976: SHELXS86, Program for Solving Crystal Structures, University of Gottingen, 1986.